Vol. 46 (2015) *ACTA PHYSICA POLONICA B* No 8

UNINTEGRATED GLUON DISTRIBUTIONS FOR FORWARD JETS AT THE LHC*

Piotr Kotko

Department of Physics, Penn State University
University Park, 16803 PA, USA

Wojciech Słomiński

The Marian Smoluchowski Institute of Physics, Jagiellonian University
Łojasiewicza 11, 30-348 Kraków, Poland

Dawid Toton

The Henryk Niewodniczański Institute of Nuclear Physics
Polish Academy of Sciences
Radzikowskiego 152, 31-342 Kraków, Poland

(Received May 27, 2015)

We test several BFKL-like evolution equations for unintegrated gluon distributions against forward–central dijet production at the LHC. Our study is based on fitting the evolution scenarios to the LHC data using the high energy factorization approach. Thus, as a by-product, we obtain a set of LHC-motivated unintegrated gluon distributions ready to use. We utilize this application by calculating azimuthal decorrelations for forward–central dijet production and compare with the existing data.

DOI:10.5506/APhysPolB.46.1527
PACS numbers: 12.38.Bx, 12.85.Hd

1. Introduction

A typical procedure in applying QCD to hadronic collisions relies on factorization theorems. They consist in two ingredients: a perturbatively calculable hard part and a nonperturbative piece parametrizing hadrons participating in a collision. The most known and tested is the collinear factorization (see *e.g.* [1] for a review), which applies for a variety of processes, including jet observables in deep inelastic scattering (DIS) and hadron–hadron

collisions. Here, the nonperturbative component is parametrized in terms of parton distribution functions (PDFs) which undergo Dokshitzer–Gribov–Lipatov–Altarelli–Parisi (DGLAP) evolution equations. The key feature of PDFs is the *universality*, *i.e.* the PDFs that are measured in one process can be used in any other for which the factorization holds. Therefore, for instance, one can use PDFs fitted to DIS structure functions and use them to make predictions for jets in hadron–hadron collisions. Although the collinear factorization is powerful and well-tested, it is supposed that for certain observables, *e.g.* forward jets at high energies, another kind of evolution equations for the PDFs is needed. Namely, the perturbative calculations contain the logarithms of the form $\alpha_{\mathrm{s}} \log(1/x)$, where x is the longitudinal fraction of the hadron momentum carried by the parton. At high energies and forward rapidities, x is small and these logarithms need to be resumed. This is accomplished by means of various "small-x" evolution equations, which essentially are various extensions of the pioneering Balitski–Fadin–Kuraev–Lipatov (BFKL) evolution equation (see *e.g.* [2]). In the small-x domain, the transverse momenta of the partons exchanged between the perturbative and nonperturbative parts are not suppressed comparing to the collinear factorization. Therefore, the PDFs have an explicit dependence on the transverse momentum of a parton. Such objects are often referred to as transverse momentum dependent PDFs (TMDs) or Unintegrated PDFs, although the former are typically used outside the small-x physics, and posses unambiguous (though, in general, process-dependent) field theoretic definitions. Actually, at small x, one usually deals with initial state gluons only, and thus the object of interest in this paper is an Unintegrated Gluon Distribution (UGD). The UGDs have to be convoluted with a perturbative "hard part" according to the so-called k_{T} or High Energy Factorization (HEF). We describe this approach in some more detail in Section 2. Here, let us just mention that unlike the collinear factorization, the HEF is not a QCD theorem and actually the universality of UGDs is supposed to be violated for jet production in hadron–hadron collisions. Thus, in principle, the standard procedure of fitting the UGDs to the F_2 HERA data and using it for jets in hadron–hadron collisions is not correct, but there are no quantitative measures of the factorization violation so far. Actually, HEF is surprisingly quite successful with describing LHC data using UGDs from fits to structure functions, see, for instance, [3]. At present, there are several fits to F_2 data using different small-x approaches, see [4–7] for more details.

In the present work we undertake another path. We make an attempt to fit various BFKL-like UGDs directly to the LHC data for forward jet production. It has a twofold purpose. First, we have an opportunity to explore UGDs using relatively exclusive observables. Second, we want to free ourselves from the aforementioned universality problem when trans-

ferring UGDs from DIS to the LHC domain. We consider two separate measurements: jet transverse momentum spectra [8] in forward–central jet production and forward–central dijet decorrelations [9]. The first measurement consists of two separate sets of data: for the forward jet and for the central jet. Thus, the mutual description of both spectra imposes a strong constraint on the UGDs and we shall use this measurements to make our fits. The second measurement will be used to test the fits.

The paper is organized as follows. In Section 2, we describe the approach of HEF. The small-x evolution equations with various components incorporating sub-leading effects are discussed in Section 3. The fitting procedure and the software used are described in Section 4. We give the results in Section 5. Having the fits, we test them against recent forward–central dijet decorrelations data in Section 6. Finally, we discuss our research in Section 7.

2. High Energy Factorization

In this introductory section, we discuss in more detail issues concerning factorization at small x. This task is somewhat complicated, notably because of the various existing approaches and various existing definitions of UGDs.

In the following paper, the notion of HEF corresponds to a general class of factorization approaches supposed to be valid at small x. Below, we list some of the existing realizations:

1. the factorization of Gribov, Levin and Ryskin (GLR) [10] for high-p_{T} inclusive gluon production;

2. the factorization of Catani, Ciafaloni and Hautmann (CCH) [11, 12] for heavy quark production in DIS, photo-production and hadron–hadron collisions;

3. the factorization of Collins and Ellis [13] for heavy quark production in hadron–hadron collisions;

4. the factorization for inclusive gluon production in the saturation regime for proton–nuclei collisions within the Color Glass Condensate (CGC) approach [14] and color dipole formalism [15, 16] (the equivalence of both approaches was shown in [17]).

In these approaches, the nonperturbative part is parametrized in terms of UGDs undergoing BFKL evolution (for GRL, CCH, Collins–Ellis factorizations) or nonlinear Balitsky–Kovchegov evolution [18, 19] (for CGC). On the other hand, superficially similar objects to UGDs appear in the so-called transverse momentum-dependent (TMD) factorization and are called TMD PDFs. One should, however, realize that the enumerated approaches are

valid at leading logarithmic approximation, while the TMD factorizations are valid to all orders in the leading twist approximation. Moreover, unlike most of UGDs in the HEF factorizations, the TMD PDFs have precise operator definitions in terms of matrix elements of nonlocal operators. Those definitions require appropriate Wilson lines to be inserted in order to make the definitions gauge-invariant and to resum collinear gluons related to final and initial state interactions. These insertions make the TMD PDFs, in general, process-dependent and thus non-universal, breaking the principle of factorization (for more details, see *e.g.* [20, 21]). Only for processes with at most two hadrons the TMD factorization is proved to hold to all orders (for example, back-to-back single hadron production in DIS or Drell–Yan scattering). The natural question arises whether the non-universality of TMD PDFs transfers to the small-x limit. In Ref. [22], an explicit arguments were given that this is the case for dilute–dense collisions (actually the arguments hold for the so-called "hybrid" factorization — see also below). Moreover, it is known from the CGC approach that at really small x, *i.e.* in the saturation regime, the cross sections cannot be described by just dipoles (averages of two Wilson lines), but also higher correlators are needed [23], what violates the ordinary logic of factorization. However, for the case of back-to-back dijet production in dilute–dense collisions, a generalized factorization has been proposed [24]; that is, the cross section can be given in terms of hard factors and certain universal pieces. Recently, these results were improved to the case of imbalanced dijets [25]. In particular, when the imbalanced transverse momentum is of the order of transverse momenta of the jets, the HEF for dijet production can be derived from the dilute limit of the CGC approach.

In the present work, we shall constrain ourselves to dijet production in p–p collisions in the linear regime, as the kinematics we are interested in (and where the data exist) do not allow to develop the saturation region. We want to utilize most of the phase space covered by the data, thus we do not constrain ourselves to the back-to-back dijet region analyzed in [24]. Rather, we shall use the HEF factorization for dijet production. Since this approach is an extension of the CCH formalism, we shall now briefly recall the latter and the required extensions to obtain HEF for dijets. For a direct derivation from CGC approach, see [25].

In the CCH high energy factorization, one considers the heavy quark pair produced via the tree-level hard sub-process $g^*(k_A)\, g^*(k_B) \to Q\overline{Q}$ in the axial gauge. The initial state gluons are off-shell and have the momenta of the form $k_A = x_A\, p_A + k_{\mathrm{T}A}$ and $k_B = x_B\, p_B + k_{\mathrm{T}B}$, where p_A, p_B are the momenta of the incoming hadrons and $p_A \cdot k_{\mathrm{T}A} = p_B \cdot k_{\mathrm{T}B} = 0$. This particular form of the exchanged momenta is a result of the imposed high energy limit. The off-shell gluons have "polarization vectors" that are p_A

and p_B respectively. Thanks to this kinematics, the sub-process given by ordinary Feynman diagrams is gauge-invariant despite its off-shellness. In CCH approach, the factorization formula for heavy quark production reads (see Fig. 1 (a))

$$d\sigma_{AB\to Q\overline{Q}} = \int d^2k_{\mathrm{T}A} \int \frac{dx_A}{x_A} \int d^2k_{\mathrm{T}B} \int \frac{dx_B}{x_B} \times \mathcal{F}_{g^*/A}\left(x_A, k_{\mathrm{T}A}\right) \mathcal{F}_{g^*/B}\left(x_B, k_{\mathrm{T}B}\right) d\hat{\sigma}_{g^*g^*\to Q\overline{Q}}\left(x_A, x_B, k_{\mathrm{T}A}, k_{\mathrm{T}B}\right) , \quad (1)$$

where $d\hat{\sigma}_{g^*g^*\to Q\overline{Q}}$ is the partonic cross section built up from the gauge-invariant $g^*g^* \to Q\overline{Q}$ amplitude and $\mathcal{F}_{g^*/A}$, $\mathcal{F}_{g^*/B}$ are UGDs for hadrons A and B. The contributions with off-shell quarks are suppressed. The UGDs are assumed to undergo the BFKL evolution equations. In Ref. [12], it was argued that similar factorization holds to all orders for DIS heavy quark structure function, although the argumentation misses the details comparing to collinear factorization proofs [1], especially the definitions of UGDs and complications arising at higher orders in the axial gauge [26].

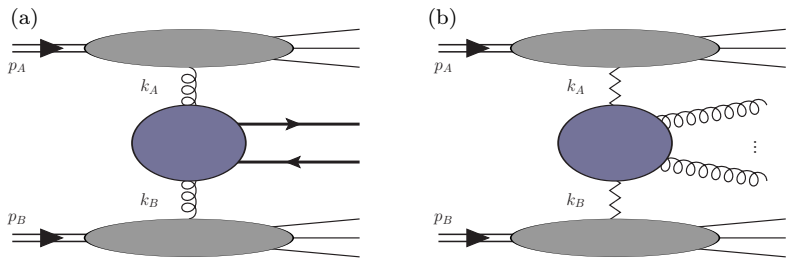

Fig. 1. (a) The CCH factorization for inclusive heavy quark production; despite the fact that the gluons entering the central blob are off-shell, the sub-process is gauge-invariant. (b) For sub-processes with final state gluons, the gauge invariance requires the off-shell gluons to be replaced by the effective particles giving rise to multiple eikonal gluon exchanges between the blobs.

In the works [3, 6, 27–30] as well as in this paper, the CCH factorization was extended to model the cross section for jet production in hadron–hadron collisions. The first difficulty arises because now one has to consider also gluons in the final state, *e.g.* $g^*g^* \to gg$ sub-process for dijet production. The corresponding amplitude is, however, not gauge-invariant when calculated from ordinary Feynman diagrams. A few approaches have been proposed to calculate a gauge-invariant extension of such amplitudes [29, 31–34]. These gauge-invariant off-shell amplitudes, in fact, correspond to a vertex that can be calculated from the well-known Lipatov's effective action [35, 36] (see Fig. 1 (b)). The approaches [29, 31–34] were, however, oriented on practical and efficient computations of multi-particle off-shell amplitudes

using helicity method and computer codes. As stated before, in CCH, the UGDs undergo BFKL evolution. In our extensions of CCH approach, we allow the UGDs to undergo more complicated evolution equations, which are more suitable for jets. More details will be given in Section 3. Yet another modification of the CCH formula comes from the fact that the present study concerns the system of dijets where one of the jet is forward, while the second is in the central region. From $2 \to 2$ kinematics, it follows then that $x_A \ll x_B$ (or the opposite), except for the small corner of the phase space. Since x_B is typically of the order of 0.5 the usage of small-x evolution for $\mathcal{F}_{g^*/B}$ is questionable (this is similar to dilute–dense system considered *e.g.* in [24]). Therefore, we use collinear approach on the B hadron side [37]. Technically, one takes the collinear limit in $d\hat{\sigma}_{g^*g^*\to 2j}$ by sending $k_{\mathrm{T}B} \to 0$ to obtain a sub-process with one off-shell gluon $d\hat{\sigma}_{g^*g\to 2j}$ (the off-shell amplitudes have well defined on-shell limit). In this limit, one has to take into account also sub-processes with initial state on-shell quarks, $d\hat{\sigma}_{g^*q\to 2j}$. The remaining integral over $d^2k_{\mathrm{T}B}$ gives helicity sum for B partons on the one hand, and the integrated (collinear) PDF on the other $\int dk_B^2\, \mathcal{F}_{a^*/B}\left(x_B, k_{\mathrm{T}B}\right) = f_a\left(x_B\right)$. Thus, the final formula for the factorization model reads

$$d\sigma_{AB\to 2j} = \int d^2k_{TA} \int \frac{dx_A}{x_A} \int \frac{dx_B}{x_B} \times \sum_b \mathcal{F}_{g^*/A}\left(x_A, k_{TA}, \mu\right)\, f_b\left(x_B, \mu\right)\, d\hat{\sigma}_{g^*b\to 2j}\left(x_A, x_B, k_{TA}, \mu\right)\,, \quad (2)$$

where we have included the hard scale dependence not only in the collinear PDFs f_b, but in the UGD as well. Such a dependence turns out to be important for certain exclusive observables involving a hard scale (*e.g.* large p_{T} of jets; see *e.g.* [3]). We note that when the final states become well separated in rapidity, *i.e.* when the central jet lies in the opposite hemisphere to the forward jet, we start to violate our condition $x_A \ll x_B$ and different approach should be used. The factorization formula (2) resembles the linearized approach of [24] but it extends beyond the correlation limit as here the hard sub-processes have injected a nonzero k_{T}. As mentioned before, formula (2) has been recently derived from the CGC approach in [25].

3. Small-x evolution equations

Let us now discuss the evolution equations for UGDs which were used in our fits. As described in the preceding section, we concentrate on linear evolution equations. Below, we list some of them with a short explanation. We consider only gluon UGDs, thus we skip the subscripts in $\mathcal{F}_{g^*/A}$.

1. Pure BFKL equation. The equation in the leading logarithmic approximation reads [38, 39]

$$\mathcal{F}\left(x,k_{\mathrm{T}}^2\right)=\mathcal{F}_0\left(x,k_{\mathrm{T}}^2\right)$$
$$+\overline{\alpha}_{\mathrm{s}}\int\limits_x^1\frac{dz}{z}\int\limits_0^\infty dq_{\mathrm{T}}^2\left[\frac{q_{\mathrm{T}}^2\mathcal{F}\left(\frac{x}{z},q_{\mathrm{T}}^2\right)-k_{\mathrm{T}}^2\mathcal{F}\left(\frac{x}{z},k_{\mathrm{T}}^2\right)}{\left|q_{\mathrm{T}}^2-k_{\mathrm{T}}^2\right|}+\frac{k_{\mathrm{T}}^2\mathcal{F}\left(\frac{x}{z},k_{\mathrm{T}}^2\right)}{\sqrt{4q_{\mathrm{T}}^4+k_{\mathrm{T}}^4}}\right], \quad (3)$$

where $\overline{\alpha}_{\mathrm{s}}=N_c\alpha_{\mathrm{s}}/\pi$ with N_c being the number of colors. The initial condition for the evolution is given by $\mathcal{F}_0$. The NLO BFKL equation is also known [40, 41]. One of the drawbacks of the pure BFKL equation comes from the fact that q_{T}^2 of the gluons emitted along the ladder is unconstrained. Indeed, since in the BFKL regime the virtuality of the exchanged gluons is dominated by the transverse components, the resulting *kinematic constraint* reads [42, 43]

$$q_{\mathrm{T}}^2<\frac{1-z}{z}\,k_{\mathrm{T}}^2\approx\frac{1}{z}\,k_{\mathrm{T}}^2\,. \quad (4)$$

This constraint is also often referred to as the consistency constraint.

2. BFKL with the kinematic constraint (BFKL+C).

To incorporate the consistency constraint, one may include the appropriate step function into the real emission part of the BFKL. This operation actually introduces some higher order corrections into the BFKL equation [43]. In addition, one may introduce another class of sub-leading corrections by allowing the strong coupling constant to run with the local scale along the ladder. Finally, one may define the q_{T}^2 integration region to lie away from the infrared nonperturbative region by separating the $\int_0^{k_{\mathrm{T0}}^2}dq_{\mathrm{T}}^2$ integration and moving it to the initial condition (the infrared cutoff k_{T0}^2 is taken to be of the order of 1 GeV). The improved equation reads [44]

$$\mathcal{F}\left(x,k_{\mathrm{T}}^2\right)=\mathcal{F}_0\left(x,k_{\mathrm{T}}^2\right)+\overline{\alpha}_{\mathrm{s}}\left(k_{\mathrm{T}}^2\right)\int\limits_x^1\frac{dz}{z}\int\limits_{k_{\mathrm{T0}}^2}^\infty dq_{\mathrm{T}}^2$$
$$\times\left[\frac{q_{\mathrm{T}}^2\mathcal{F}\left(\frac{x}{z},q_{\mathrm{T}}^2\right)\Theta\left(k_{\mathrm{T}}^2-zq_{\mathrm{T}}^2\right)-k_{\mathrm{T}}^2\mathcal{F}\left(\frac{x}{z},q_{\mathrm{T}}^2\right)}{\left|q_{\mathrm{T}}^2-k_{\mathrm{T}}^2\right|}+\frac{k_{\mathrm{T}}^2\mathcal{F}\left(\frac{x}{z},k_{\mathrm{T}}^2\right)}{\sqrt{4q_{\mathrm{T}}^4+k_{\mathrm{T}}^4}}\right]. \quad (5)$$

Recently, it has been studied in the context of the Mueller–Navelet jets that the energy-momentum conservation violation (which above is cured by a "brute force") becomes less harmful when full NLO corrections are applied [45]. The effects of the kinematic constraints in the approximate form (4) as well as in the full form have been recently analyzed [46] in the context of the CCFM evolution equation [47–50].

3. BFKL with the kinematic constraint in the resummed form (BFKL+CR).

   Equation (5) can be casted in yet another form [51]

$$\mathcal{F}\left(x,k_{\mathrm{T}}^2\right)=\tilde{\mathcal{F}}_0\left(x,k_{\mathrm{T}}^2\right)+\overline{\alpha}_{\mathrm{s}}\left(k_{\mathrm{T}}^2\right)$$
$$\times\int\limits_x^1\frac{dz}{z}\int\limits_{k_{\mathrm{T}0}^2}^{\infty}\frac{d^2q_{\mathrm{T}}}{\pi q_{\mathrm{T}}^2}\Theta\left(q_{\mathrm{T}}^2-\mu^2\right)\Delta_{\mathrm{R}}\left(z,k_{\mathrm{T}}^2,\mu^2\right)\mathcal{F}\left(\frac{x}{z},\left|\vec{k}_{\mathrm{T}}+\vec{q}_{\mathrm{T}}\right|^2\right),\quad(6)$$

   where

$$\Delta_{\mathrm{R}}\left(z,k_{\mathrm{T}}^2,\mu^2\right)=\exp\left(-\overline{\alpha}_{\mathrm{s}}\ln\frac{1}{z}\ln\frac{k_{\mathrm{T}}^2}{\mu^2}\right)\quad(7)$$

   is the so-called Regge form factor. This form has been used in Ref. [51] to propose a non-linear extension of the CCFM equation. The scale μ has been introduced to separate unresolved and resolved emissions in (5), *i.e.* the emissions with $q_{\mathrm{T}}^2<\mu^2$ and $q_{\mathrm{T}}^2>\mu^2$, and further the unresolved part was resummed to obtain the Regge form factor. Note that the UGDs undergoing this equation do not explicitly depend on the scale μ and that the new form of the initial condition has to be used (this is denoted by a tilde sign).

4. BFKL with the kinematic constraint and DGLAP correction (BFKL+CD).

   In Ref. [44] yet another improvement of (3) was proposed. One can make an attempt to account for DGLAP-like behavior by including the non-singular part of the gluon splitting function (the third term below)

$$\mathcal{F}\left(x,k_{\mathrm{T}}^2\right)=\mathcal{F}_0\left(x,k_{\mathrm{T}}^2\right)+\overline{\alpha}_{\mathrm{s}}\left(k_{\mathrm{T}}^2\right)\int\limits_x^1\frac{dz}{z}\int\limits_{k_{\mathrm{T0}}^2}^{\infty}dq_{\mathrm{T}}^2$$

$$\times\left[\frac{q_{\mathrm{T}}^2\mathcal{F}\left(\frac{x}{z},q_{\mathrm{T}}^2\right)\Theta\left(k_{\mathrm{T}}^2-zq_{\mathrm{T}}^2\right)-k_{\mathrm{T}}^2\mathcal{F}\left(\frac{x}{z},q_{\mathrm{T}}^2\right)}{\left|q_{\mathrm{T}}^2-k_{\mathrm{T}}^2\right|}+\frac{k_{\mathrm{T}}^2\mathcal{F}\left(\frac{x}{z},k_{\mathrm{T}}^2\right)}{\sqrt{4q_{\mathrm{T}}^4+k_{\mathrm{T}}^4}}\right]$$

$$+\overline{\alpha}_{\mathrm{s}}\left(k_{\mathrm{T}}^2\right)\int\limits_x^1\frac{dz}{z}\left(\frac{z}{2N_c}P_{gg}\left(z\right)-1\right)\int\limits_{k_{\mathrm{T0}}^2}^{k_{\mathrm{T}}^2}dq_{\mathrm{T}}^2\mathcal{F}\left(\frac{x}{z},q_{\mathrm{T}}^2\right),\qquad(8)$$

where $P_{gg}\left(z\right)$ is the standard gluon splitting function. This correction, similar to the kinematic constraint, accounts for certain sub-leading corrections to the BFKL equation.

5. BFKL with DGLAP correction alone.

   This variant is used to test the significance of the DGLAP term alone.

The above UGDs do not involve any hard scale dependence. For observables involving high-p_{T} jets, a presence of large scale $\mu^2\sim p_{\mathrm{T}}^2$ in perturbative calculations would involve additional logarithms of the type $\log\left(\mu^2/k_{\mathrm{T}}^2\right)$ which can spoil the procedure. Therefore, a resummation of those logs is desired and it accounts in hard scale dependence for UGDs, *cf.* Eq. (2). The approach which incorporates both x, k_{T}^2 and μ^2 dependence in UGDs is provided, for example, by the CCFM evolution equation (the code available for a practical use is described, for example, in [52]). Another approach, the so-called KMR (Kimber–Martin–Ryskin) procedure [53, 54], takes ordinary PDFs and injects k_{T} dependence via the Sudakov form factor taking care of matching to the BFKL evolution at small x. A serious advantage of this procedure is that one can use well known PDF sets, fitted to large data sets. Yet another approach was used in [3] in therms of the so-called "Sudakov resummation model". This procedure reverts, in a sense, the logic used in the KMR and uses the Sudakov form factor to inject the hard scale dependence instead of k_{T}. The procedure is parton-shower-like, *i.e.* it is applied after the MC events are generated and the cross section is known, and is unitary (*i.e.* the procedure does not change the total cross section). The advantage is that one may use it on the top of UGDs involving nonlinear effects. The basic idea behind the model is that it assigns the Sudakov probability P for events with given k_{T} and a hard scale $\mu\sim p_{\mathrm{T}}$. Then, the probability of surviving is $1-P$. For events with small k_{T} and large μ, the emission probability is $P\sim 1$ and the unitarity of the procedure transfers such events to the region $k_{\mathrm{T}}\sim p_{\mathrm{T}}$. There is one more approach proposed in Ref. [55],

similar to the one just described, where analogous procedure is applied at the level of UGDs by fixing its integral over k_{T} (it has an advantage of being independent on any software and one may produce grids for a practical usage). In summary, we may consider the following modifications of UGDs 1–5:

6. BFKL with the Sudakov (BFKL+S).
7. BFKL with the kinematic constraint and the Sudakov (BFKL+CS).
8. BFKL with DGLAP correction and the Sudakov (BFKL+DS).
9. BFKL with the kinematic constraint in resummed form and the Sudakov (BFKL+CRS).
10. BFKL with the kinematic constraint, DGLAP correction and the Sudakov (BFKL+CDS).

Unfortunately, as far as fitting of UGDs is considered, the above Sudakov-based models are not suitable. This is because they require the knowledge of an integral (whether it is a cross section or integrated gluon, *cf.* [3] *vs.* [55]) which is unknown at the stage of fitting. In principle, one could try to use the method of successive approximations with the Sudakov model of Ref. [3]. We shall report on our attempts in Section 5. There is one more comment in order here. The Sudakov resummation model is very sensitive to the region $k_{\mathrm{T}} \lesssim 1$ GeV which is not well described by the practical implementations of the equations in 1–5 as they use certain low-k_{T} cut, k_{T0}. For $k_{\mathrm{T}} < k_{\mathrm{T0}}$, the UGD is typically modeled or extrapolated by a constant value.

Let us now discuss the models for the initial condition $\mathcal{F}_0$. In this paper, we have tested the following models (in the brackets we give the aliases used below to identify the model):

A. exponential model (EXP)

$$\mathcal{F}_0\left(x, k_{\mathrm{T}}^2\right) = N\, e^{-Ak_{\mathrm{T}}^2} (1-x)^a (1 - Dx) \; ; \tag{9a}$$

B. (negative) power-like model with running α_{s} (POW)

$$\mathcal{F}_0\left(x, k_{\mathrm{T}}^2\right) = \frac{\overline{\alpha}_{\mathrm{s}}\left(k_{\mathrm{T}}^2\right)}{k_{\mathrm{T}}^2} N\, x^A (1-x)^a (1 - Dx) \, ; \tag{9b}$$

C. DGLAP-based model (Pgg)

$$\mathcal{F}_0\left(x, k_{\mathrm{T}}^2\right) = \frac{\alpha_{\mathrm{s}}\left(k_{\mathrm{T}}^2\right)}{2\pi k_{\mathrm{T}}^2} \int\limits_x^1 dz\, P_{gg}(z)\, \hat{\mathcal{G}}_0(x) \; , \tag{9c}$$

where

$$\hat{\mathcal{G}}_0(x) = N\, x^A (1-x)^a (1-Dx) \tag{9d}$$

is a model for an integrated gluon density.

The parameters N, A, a, D are, in general, free parameters and need to be fitted.

We see that, in principle, there are quite a few variants to be fitted. Though not all of the combinations make sense, we are still left with several scenarios to be tested.

4. Fitting procedure

We have used two data samples measured by CMS detector [8] for inclusive forward–central dijet production at CM energy $\sqrt{s} = 7$ TeV. The central jet is defined to lie within the pseudo-rapidity interval $|\eta_c| < 2.8$, while the forward has to lie within $4.9 > |\eta_f| > 3.2$. Both jets are high-p_{T} jets with $p_{\mathrm{T}} > 35$ GeV. The jets were reconstructed using anti-k_{T} algorithm with radius $R = 0.5$. The data samples consist in jet p_{T} spectra for forward and for central jets, $d\sigma_S/dp_{\mathrm{T}}\Delta\eta_S$ with $S = f, c$. There are in total 12 data bins for both forward and central jets.

We have applied the following fitting procedure. For each existing experimental data bin B, we produce a 2-dimensional normalized histogram $\mathcal{H}^B$ with bins in x and k_{T}, such that the cross section can be calculated as

$$\sigma^B = \sum_{i,j} \mathcal{H}^B_{ij} \mathcal{F}\left(x\left(i\right), k_{\mathrm{T}}\left(j\right)\right), \tag{10}$$

where i, j enumerate the bins in (x, k_{T}). To make the histograms $\mathcal{H}^B$, we

1. generate Monte Carlo events for the process under consideration with $\mathcal{F} = \mathcal{F}^*$, where $\mathcal{F}^*$ is a relatively "broad" trial UGD (evolving according to one of the scenarios 1–10),
2. make histograms $\mathfrak{h}^B$ in (x, k_{T}) of contributions to each data bin B,
3. divide by $\mathcal{F}^*(x, k_{\mathrm{T}})$, *i.e.* $\mathcal{H}^B_{ij} = \mathfrak{h}^B_{ij}/\mathcal{F}^*\left(x\left(i\right), k_{\mathrm{T}}\left(j\right)\right)$.

Hence, in principle, $\mathcal{H}^B$ are independent of $\mathcal{F}^*$ used for their generation and are calculated only once. This is advantageous as the hard cross section calculation is costly in CPU time. The latter is calculated using the Monte Carlo `C++` program `LxJet` [56] implementing (2). The generated events (weighted or unweighted) are stored in a `ROOT` [57] file for further processing. For the UGD evolution according to scenarios 1–5, we solve the corresponding integral equations by a straightforward numerical iteration over a grid over x and k_{T}.

In order to make the fitting feasible, we need a fast routine to calculate $\mathcal{F}$ used in (10) for the cross section calculation. However, since our numerical procedure is too slow for that, we prepare grids over which we can interpolate the fitting parameters. Each such grid corresponds to a particular parametrization model and arguments range. Out of four parameters (N, A, a, D) of the initial conditions, we fix $D = 0$ (see Sec. 5). Moreover, we note that the solution for $\mathcal{F}$ is linear in N. Thus, the actual grids are in A and a.

5. Results

We have applied the procedure described in the preceding section to most of the models 1–10 and initial conditions A–C. The best values of χ^2/NDP (χ^2 per data point) are listed in Table I for models 1–5. Note, that some of the scenarios were unable to describe the data, in particular the pure BFKL and BFKL with the kinematic constraint only. Evidently, the DGLAP correction is essential. The fitted values of the parameters of the initial conditions, N, A, a, for scenarios with χ^2/NDP < 2 are collected in Table II. The fits are presented in Figs. 2 and 3. For a better comparison, we also plot the cross sections scaled by p_{T}^5. We observe that all the models with the DGLAP correction give excellent description of the central-jet data, while the p_{T} spectrum of forward jets is reasonably reproduced though less accurately. We also note that the models with lowest χ^2 result in very similar predictions for the p_{T} spectra.

TABLE I

The values of χ^2/NDP for fits of unintegrated gluon density evolving according to various models described in Section 3. The first column lists the initial condition ansatz, see also Section 3 for details.

$\mathcal{F}_0$	BFKL	BFKL+C	BFKL+D	BFKL+CD	BFKL+CR
EXP	2.4	2.2	1.24	1.11	1.52
POW	2.3	1.9	1.02	1.12	—
Pgg	—	—	1.13	1.11	—

Our attempts to fit the scenarios with the Sudakov resummation can be summarized as follows. First, we observe that the model has a small overall effect on the p_{T} spectra, although it slightly shifts the theory points away from the data points. We illustrate this in Fig. 4, where we applied the Sudakov model on the top of the events obtained with one of the fits. When we now try to refit the $\mathcal{F}_0$ parameters, we change the total cross section (used already to apply the resummation) and the fit fails. Although we observe that the successive iterations improve the fit, the procedure turns out to be insufficient to make a reliable fit with the Sudakov resummation.

TABLE II

The values of initial condition A–C parameters obtained from the fits to the CMS data. We list only the scenarios with $\chi^2/\mathrm{NDP} < 2$. The values denoted by a star were fixed — see the main text for details.

Model	N	A	a
BFKL+CR (EXP)	0.095	0.012	0*
BFKL+D (EXP)	0.37	0.18	0.5*
BFKL+CD (EXP)	0.68	0.14	2.5*
BFKL+C (POW)	320	1.4	61.0
BFKL+D (POW)	12.7	0.5*	5.7
BFKL+CD (POW)	562	0.96	35.7
BFKL+D (Pgg)	106	1.2	2.5
BFKL+CD (Pgg)	628	2.9	5.7

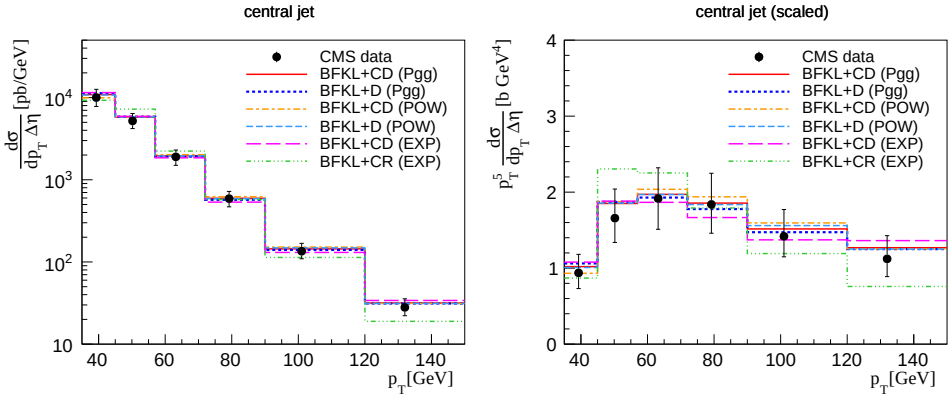

Fig. 2. The p_{T} spectra of the central jet calculated using the best fits for individual models *versus* the CMS data. For the right plot, the cross sections have been scaled by p_{T}^5 to better see the differences between the models.

A few comments are in order. The considered jet data are not sufficient to precisely determine all the parameters (N, A, a, D) of the initial parametrizations (9). Thus, first, we neglect the $(1 - Dx)$ factor, *i.e.* we take $D = 0$. We have checked that we get no improvement when D is a free parameter. Next, in some cases, the fits are not sensitive enough to uniquely determine the three remaining free parameters. In these cases, we fix A or a at some plausible value (these are marked with a star in Table II). Actually, besides the initial condition parameters N, A, a, D, we have also the boundary values of kinematic parameters x_A, k_{T} (*cf.* (2)), which — to certain extent — are free parameters as well. We set them as follows. First, in order to be in accordance with the assumptions leading to (2), we imply

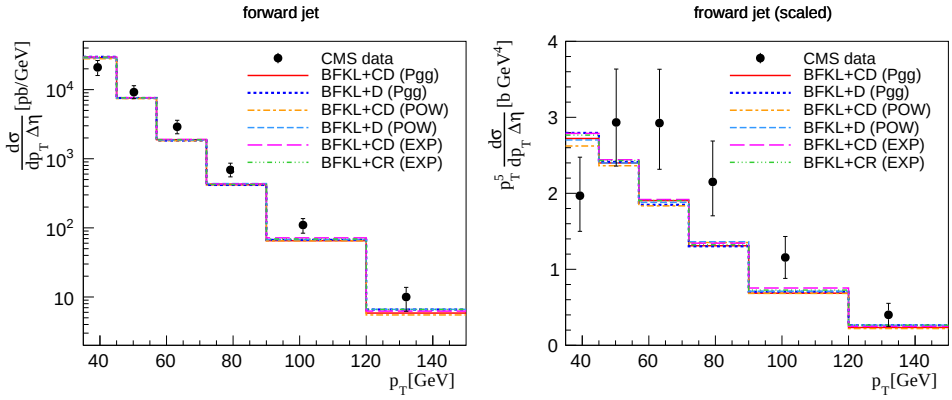

Fig. 3. The p_{T} spectra of the forward jet calculated using the best fits for individual models *versus* the CMS data. For the right plot, the cross sections have been scaled by p_{T}^5 to better see the differences between the models.

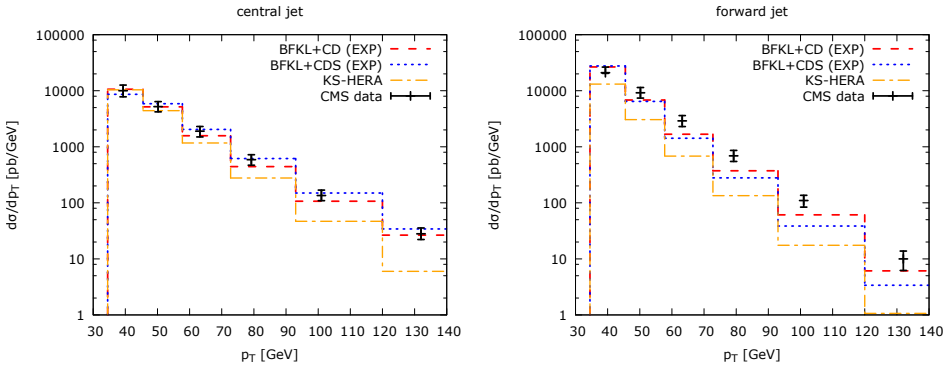

Fig. 4. An effect of the Sudakov resummation model (BFKL+CDS) when applied to one of our fits for the model BFKL+CD with exponential initial condition. For comparison, we plot also the spectra obtained from the unintegrated gluon density with more involved evolution and fitted to HERA data (KS-HERA), see the text for more details.

the cut $x_A < x_B$. Next, for all scenarios, we set $x_{A\,\mathrm{min}} = 0.0001$. For the model with the DGLAP correction, we set $x_{A\,\mathrm{max}} = 1.0$, while for the others we set $x_{A\,\mathrm{max}} = 0.4$. Further, we use $k_{\mathrm{T\,min}} = 1$ GeV for DGLAP models and $k_{\mathrm{T\,min}} = 0.1$ GeV for the others. Finally, we use $k_{\mathrm{T\,max}} = 100$ GeV for exponential initial condition and $k_{\mathrm{T\,max}} = 400$ GeV for the others. The last comment concerns the hard scale choice: in all fits, we have used the average p_{T} of the jets.

The influence of the Sudakov resummation model is illustrated in Fig. 4. Here, we have chosen the best fits to illustrate the effect. We see that the jet spectra are rather weakly affected by the resummation, although the forward jet spectrum becomes steeper than the data.

The obtained UGDs are plotted in one-dimensional plots in Fig. 5 as a function of x and k_{T}. Note that in order to better reflect the difference between UGDs, we plot $k_{\mathrm{T}}^2 \mathcal{F}(x, k_{\mathrm{T}})$. We show results of all the models of Table II, hence also those with rather high χ^2 value (see Table I).

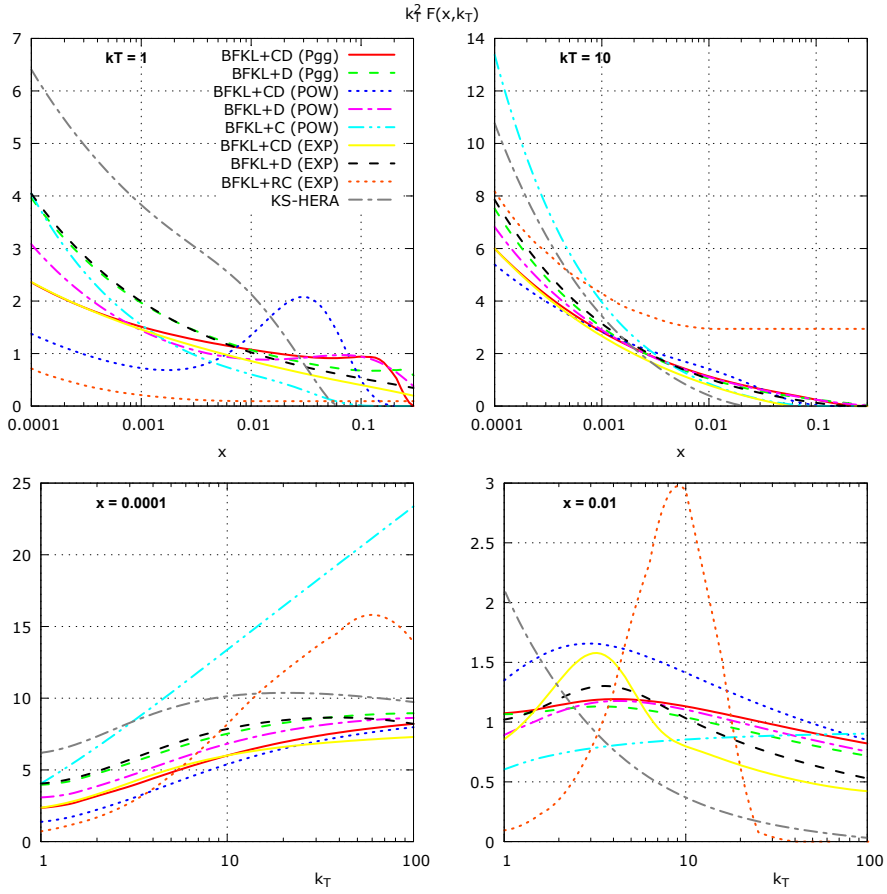

Fig. 5. Unintegrated gluon distributions evolving due to the models 1–5 with the initial conditions A–C obtained from the fits to the LHC data as a function of x (top) and k_{T} (bottom). The UGDs are multiplied by k_{T}^2 to better illustrate the differences between the models. The most differing UGDs are those without the DGLAP correction and with significantly higher $\chi^2/\mathrm{NDP} > 1.5$ (BFKL+C and BFKL+RC).

All the UGDs with the DGLAP contribution are comparable, which shows that the evolution scenario is more important than a particular shape of the initial parametrization. On the other hand, the differences between UGDs are more pronounced than those in the p_{T} spectra, which means that the currently available data are not sufficient to discriminate among the models. The two most differing UGDs correspond to the BFKL+C (POW) and BFKL+CR (EXP) models which, however, have significantly higher χ^2/NDP (above 1.5).

We compare the new LHC-based UGDs with the one evolving according to a complicated evolution of [44, 58] and fitted to the HERA data [6] (we abbreviate it as 'KS-HERA' in the figure). This evolution equation contains the kinematic constraint, full DGLAP correction (including quarks via coupled equations) and a nonlinear term motivated by the Balitsky–Kovchegov equation. The p_{T} spectra resulting from this gluon density are presented in Fig. 4.

6. Azimuthal decorrelations

In order to apply the fits in practice, we have calculated another observable for central–forward dijet production, namely, the differential cross sections in azimuthal angle $\Delta\phi$ between the two jets. At leading order, the two jets are produced exactly back-to-back and the distribution is the Dirac delta at $\Delta\phi = \pi$. However, due to QCD emissions of additional partons (either forming additional jets or being soft particles with small p_{T}), the two jets are decorrelated. On the theory side, these decorrelations are well described by QCD-based parton shower algorithms. However, within the HEF, there is a natural decorrelation mechanism built-in. Namely, due to the internal transverse momentum k_{T} of a gluon, the dijet system with transverse momenta $\vec{p}_{\mathrm{T}1}$, $\vec{p}_{\mathrm{T}2}$ is unbalanced by the amount $|\vec{p}_{\mathrm{T}1} + \vec{p}_{\mathrm{T}1}| = \left|\vec{k}_{\mathrm{T}}\right| = k_{\mathrm{T}}$. One can think of k_{T} as a cumulative transverse momentum of many gluon emissions. In general, these emissions can be small-p_{T} and large-p_{T} emissions as well. The large-p_{T} emissions may, in general, result in a jet, thus we consider inclusive dijet observables.

Using the new fits and the `LxJet` program, we have calculated the azimuthal decorrelations for the kinematics described in the beginning of Section 4. The results are presented in Fig. 6. The bands represent uncertainty that comes from the scale variation by a factor of two. We compare our calculation with the preliminary CMS data [9][1].

[1] We note that the total cross section obtained from [9] does not agree with [8]. The ratio of the two is approx. 1.8. If this is a normalization difference only, our predictions should be shifted up by this factor.

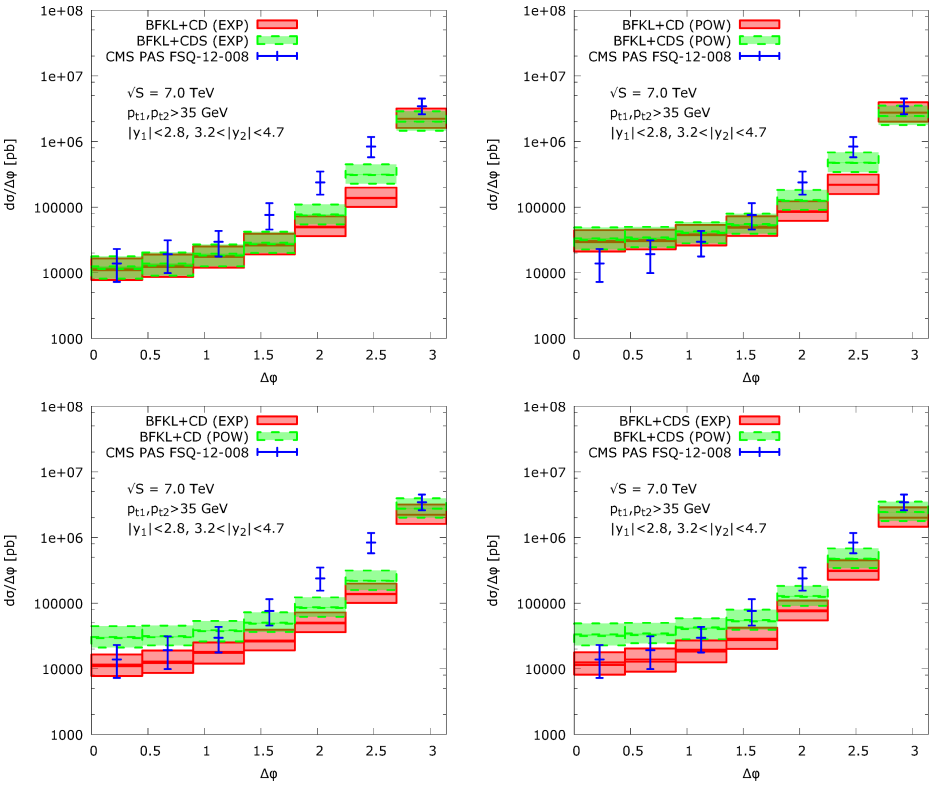

Fig. 6. The results for the azimuthal decorrelations for inclusive forward–central dijet production using our best fits. When the Sudakov resummation model is applied to the generated events, we get a better description of the CMS data.

7. Discussion

In the present paper, we went through a thorough study of various small-x evolution equations analyzing an impact of various effects on jet observables. The effects we mean here are certain sub-leading corrections to the BFKL equation, such as the kinematic constraint or DGLAP corrections. Our study was based on fitting these evolution scenarios to two samples of LHC data for high-p_{T} spectra for dijet production. These samples consist of separate spectra for the central rapidity and forward rapidity jets.

Our findings can be summarized as follows. First observation is that both forward jet and central jet spectra can be simultaneously and reasonably described by the High Energy Factorization approach and BFKL-like evolution. We obtain the best quality fits for BFKL with DGLAP correction and kinematic constraint, with the DGLAP correction being the most important additional ingredient. This matches the fact that the data under

consideration can be nicely described by the collinear factorization with a parton shower [8, 9], whereas in the High Energy Factorization, the parton shower is — to some extent — simulated by the transverse momentum-dependent gluon distribution with the DGLAP correction. For all evolution models, we get very good fits to the central jet spectrum, while most of the models have problems with precise reproduction of the shape of the forward jet spectrum. Several models properly describe the dijet data despite some differences in the resulting UGDs. Measurements of some other observables or more differential dijet data could help to discriminate among the models.

Using our fits, we have calculated azimuthal decorrelations for the same kinematic domain. This observable was also measured by CMS. The comparison of our calculation with the data is reasonably good, especially when using the Sudakov resummation model on the top of the evolution models. Interestingly, the same resummation procedure spoils the forward jet p_{T} spectrum.

Our final remark is that although the High Energy Factorization with improved BFKL evolution equation catches the main physical aspects of the jet production at small x, one definitely needs higher order corrections. Such calculations exist for certain small-x processes like Mueller–Navelet jets [45, 59] or inclusive hadron production $p + A$ collisions within CGC formalism [60, 61], but not for the high-p_{T} dijet observables under consideration.

We thank K. Kutak and A. van Hameren for many fruitful discussions. The work of P.K. and W.S. has been supported by the Polish National Science Center Grant No. DEC-2011/03/B/ST2/00220. D.T. has been supported by NCBiR Grant No. LIDER/02/35/L-2/10/NCBiR/2011. P.K. also acknowledges the support of D.O.E. grants No. DE-SC-0002145 and DE-FG02-93ER40771.

REFERENCES

[1] J. Collins, *Foundations of Perturbative QCD*, Cambridge Univ. Press, 2011.

[2] L.N. Lipatov, *Phys. Rep.* **286**, 131 (1997) [arXiv:hep-ph/9610276].

[3] A. van Hameren, P. Kotko, K. Kutak, S. Sapeta, *Phys. Lett. B* **737**, 335 (2014) [arXiv:1404.6204 [hep-ph]].

[4] J. Ellis, H. Kowalski, D.A. Ross, *Phys. Lett. B* **668**, 51 (2008) [arXiv:0803.0258 [hep-ph]].

[5] D.A. Ross, H. Kowalski, L.N. Lipatov, G. Watt, *AIP Conf. Proc.* **1350**, 47 (2011).

[6] K. Kutak, S. Sapeta, *Phys. Rev. D* **86**, 94043 (2012) [arXiv:1205.5035 [hep-ph]]

[7] A.V. Lipatov, G.I. Lykasov, N.P. Zotov, *Phys. Rev. D* **89**, 14001 (2014) [arXiv:1310.7893 [hep-ph]].

[8] S. Chatrchyan *et al.* [CMS Collaboration], *J. High Energy Phys.* **1206**, 36 (2012) [arXiv:1202.0704 [hep-ex]].

[9] S. Chatrchyan *et al.* [CMS Collaboration], "Measurement of Azimuthal Correlations Between Forward and Central Jets in Proton–Proton Collisions at $\sqrt{(s)} = 7$ TeV", CMS-PAS-FSQ-12-008.

[10] L.V. Gribov, E.M. Levin, M.G. Ryskin, *Phys. Rep.* **100**, 1 (1983), http://www.sciencedirect.com/science/article/pii/0370157383900224

[11] S. Catani, M. Ciafaloni, F. Hautmann, *Nucl. Phys. B* **366**, 135 (1991).

[12] S. Catani, F. Hautmann, *Nucl. Phys. B* **427**, 475 (1994) [arXiv:hep-ph/9405388].

[13] J.C. Collins, R.K. Ellis, *Nucl. Phys. B* **360**, 3 (1991).

[14] J.P. Blaizot, F. Gelis, R. Venugopalan, *Nucl. Phys. A* **743**, 13 (2004) [arXiv:hep-ph/0402256].

[15] Y.V. Kovchegov, K. Tuchin, *Phys. Rev. D* **65**, 74026 (2002) [arXiv:hep-ph/0111362].

[16] N. Nikolaev, W. Schafer, *Phys. Rev. D* **71**, 014023 (2005) [arXiv:hep-ph/0411365].

[17] E. Iancu, A.H. Mueller, *Nucl. Phys. A* **730**, 460 (2004) [arXiv:hep-ph/0308315].

[18] I. Balitsky, *Nucl. Phys. B* **463**, 99 (1996) [arXiv:hep-ph/9509348].

[19] Y.V. Kovchegov, *Phys. Rev. D* **60**, 34008 (1999) [arXiv:hep-ph/9901281].

[20] C.J. Bomhof, P.J. Mulders, F. Pijlman, *Eur. Phys. J. C* **47**, 147 (2006) [arXiv:hep-ph/0601171].

[21] P.J. Mulders, T.C. Rogers, arXiv:1102.4569 [hep-ph].

[22] B.W. Xiao, F. Yuan, *Phys. Rev. Lett.* **105**, 62001 (2010) [arXiv:1003.0482 [hep-ph]].

[23] F. Dominguez, C. Marquet, A.M. Stasto, B.W. Xiao, *Phys. Rev. D* **87**, 34007 (2013) [arXiv:1210.1141 [hep-ph]].

[24] F. Dominguez, C. Marquet, B.W. Xiao, F. Yuan, *Phys. Rev. D* **83**, 105005 (2011) [arXiv:1101.0715 [hep-ph]].

[25] P. Kotko *et al.*, arXiv:1503.03421 [hep-ph].

[26] E. Avsar, arXiv:1203.1916 [hep-ph].

[27] M. Deak, F. Hautmann, H. Jung, K. Kutak, arXiv:1012.6037 [hep-ph].

[28] A. van Hameren, P. Kotko, K. Kutak, *Phys. Rev. D* **88**, 094001 (2013) [arXiv:1308.0452 [hep-ph]].

[29] A. van Hameren, P. Kotko, K. Kutak, *J. High Energy Phys.* **1301**, 078 (2013) [arXiv:1211.0961 [hep-ph]].

[30] A. van Hameren *et al.*, *Phys. Rev. D* **89**, 94014 (2014) [arXiv:1402.5065 [hep-ph]].

[31] A. van Hameren, P. Kotko, K. Kutak, *J. High Energy Phys.* **1212**, 029 (2012) [arXiv:1207.3332 [hep-ph]].

[32] A. van Hameren, K. Kutak, T. Salwa, *Phys. Lett. B* **727**, 226 (2013) [arXiv:1308.2861 [hep-ph]].

[33] A. van Hameren, *J. High Energy Phys.* **1407**, 138 (2014) [arXiv:1404.7818 [hep-ph]].

[34] P. Kotko, *J. High Energy Phys.* **1407**, 128 (2014) [arXiv:1403.4824 [hep-ph]].

[35] L.N. Lipatov, *Nucl. Phys. B* **452**, 369 (1995) [arXiv:hep-ph/9502308].

[36] E.N. Antonov, L.N. Lipatov, E.A. Kuraev, I.O. Cherednikov, *Nucl. Phys. B* **721**, 111 (2005) [arXiv:hep-ph/0411185].

[37] M. Deak, F. Hautmann, H. Jung, K. Kutak, *J. High Energy Phys.* **0909**, 121 (2009) [arXiv:0908.0538 [hep-ph]].

[38] V.S. Fadin, E.A. Kuraev, L.N. Lipatov, *Phys. Lett. B* **60**, 50 (1975).

[39] E.A. Kuraev, L.N. Lipatov, V.S. Fadin, *Sov. Phys. JETP* **45**, 199 (1977).

[40] V.S. Fadin, L.N. Lipatov, *Phys. Lett. B* **429**, 127 (1998) [arXiv:hep-ph/9802290].

[41] M. Ciafaloni, G. Camici, *Phys. Lett. B* **430**, 349 (1998) [arXiv:hep-ph/9803389].

[42] B. Andersson, G. Gustafson, H. Kharraziha, J. Samuelsson, *Z. Phys. C* **71**, 613 (1996).

[43] J. Kwiecinski, A.D. Martin, P.J. Sutton, *Z. Phys. C* **71**, 585 (1996) [arXiv:hep-ph/9602320].

[44] J. Kwiecinski, A.D. Martin, A.M. Stasto, *Phys. Rev. D* **56**, 3991 (1997) [arXiv:hep-ph/9703445].

[45] B. Ducloué, L. Szymanowski, S. Wallon, *Phys. Lett. B* **738**, 311 (2014) [arXiv:1407.6593 [hep-ph]].

[46] M. Deak, K. Kutak, *J. High Energy Phys.* **1505**, 068 (2015) [arXiv:1503.00536 [hep-ph]].

[47] M. Ciafaloni, *Nucl. Phys. B* **296**, 49 (1988).

[48] S. Catani, F. Fiorani, G. Marchesini, *Phys. Lett. B* **234**, 339 (1990).

[49] S. Catani, F. Fiorani, G. Marchesini, *Nucl. Phys. B* **336**, 18 (1990).

[50] G. Marchesini, *Nucl. Phys. B* **445**, 49 (1995).

[51] K. Kutak, K. Golec-Biernat, S. Jadach, M. Skrzypek, *J. High Energy Phys.* **1202**, 117 (2012) [arXiv:1111.6928 [hep-ph]].

[52] F. Hautmann, H. Jung, S.T. Monfared, *Eur. Phys. J. C* **74**, 3082 (2014) [arXiv:1407.5935 [hep-ph]].

[53] M.A. Kimber, A.D. Martin, M.G. Ryskin, *Eur. Phys. J. C* **12**, 655 (2000) [arXiv:hep-ph/9911379].

[54] M.A. Kimber, A.D. Martin, M.G. Ryskin, *Phys. Rev. D* **63**, 114027 (2001) [arXiv:hep-ph/0101348].

[55] K. Kutak, *Phys. Rev. D* **91**, 34021 (2015) [arXiv:1409.3822 [hep-ph]].

[56] P. Kotko, "LxJet", http://annapurna.ifj.edu.pl/∼pkotko/LxJet.html

[57] R. Brun, F. Rademakers, *Nucl. Instrum. Methods A* **389**, 81 (1997).

[58] K. Kutak, A.M. Stasto, *Eur. Phys. J. C* **41**, 343 (2005) [arXiv:hep-ph/0408117].

[59] B. Ducloue, L. Szymanowski, S. Wallon, *J. High Energy Phys.* **1305**, 96 (2013) [arXiv:1302.7012 [hep-ph]].

[60] G.A. Chirilli, B.W. Xiao, F. Yuan, *Phys. Rev. D* **86**, 54005 (2012) [arXiv:1203.6139 [hep-ph]].

[61] A.M. Stasto, B.W. Xiao, D. Zaslavsky, *Phys. Rev. Lett.* **112**, 012302 (2014) [arXiv:1307.4057 [hep-ph]].